Inorganic Chemistry
Article
Cite This: Inorg. Chem. XXXX, XXX, XXX−XXX
pubs.acs.org/IC

Versatile Rh- and Ir-Based Catalysts for CO_2 Hydrogenation, Formic Acid Dehydrogenation, and Transfer Hydrogenation of Quinolines

Jairo Fidalgo,[†,#] Margarita Ruiz-Castañeda,[‡,#] Gabriel García-Herbosa,[†] Arancha Carbayo,[†] Félix A. Jalón,[‡] Ana M. Rodríguez,[§] Blanca R. Manzano,*[,‡] and Gustavo Espino*[,†]

[†]Departamento de Química, Facultad de Ciencias, Universidad de Burgos, Plaza Misael Bañuelos s/n, 09001, Burgos, Spain
[‡]Departamento de Química Inorgánica, Orgánica y Bioquímica, Facultad de Químicas, IRICA, Universidad de Castilla-La Mancha, Avda. Camilo J. Cela 10, 13071 Ciudad Real, Spain
[§]Departamento de Química Inorgánica, Orgánica y Bioquímica, Escuela Técnica Superior de Ingenieros Industriales, Avda. C. J. Cela, 3, 13071 Ciudad Real, Spain

Supporting Information

ABSTRACT: Considering the interest in processes related to hydrogen storage such as CO_2 hydrogenation and formic acid (FA) decomposition, we have synthesized a set of Ir, Rh, or Ru complexes to be tested as versatile precatalysts in these reactions. In relation with the formation of H_2 from FA, the possible applicability of these complexes in the transfer hydrogenation (TH) of challenging substrates as quinoline derivatives using FA/formate as hydrogen donor has also been addressed. Bearing in mind the importance of secondary coordination sphere interactions, N,N′ ligands containing NH_2 groups, coordinated or not to the metal center, were used. The general formula of the new complexes are [(*p*-cymene)RuCl(N,N′)]X, X = Cl^-, BF_4^- and [Cp*MCl(N,N′)]Cl, M = Rh, Ir, where the N,N′ ligands are 8-aminoquinoline (HL1), 6-pyridyl-2,4-diamine-1,3,5-triazine (L2) and 5-amino-1,10-phenanthroline (L3). Some complexes are not active or catalyze only one process. However, the complexes [Cp*MCl(HL1)]Cl with M = Rh, Ir are versatile catalysts that are active in hydrogenation of quinolines, FA decomposition, and also in CO_2 hydrogenation with the iridium derivative being more active and robust. The CO_2 hydrogenation takes place in mild conditions using only 5 bar of pressure of each gas (CO_2 and H_2). The behavior of some precatalysts in D_2O and after the addition of 9 equiv of HCO_2Na (pseudocatalytic conditions) has been studied in detail and mechanisms for the FA decomposition and the hydrogenation of CO_2 have been proposed. For the Ru, Ir, or Rh complexes with ligand HL1, the amido species with the deprotonated ligand are observed. In the case of ruthenium, the formate complex is also detected. For the iridium derivative, both the amido intermediate and the hydrido species have been observed. This hydrido complex undergoes a process of umpolung $D^+ \leftrightarrow$ Ir−D. All in all, the results of this work reflect the active role of $-NH_2$ in the transfer of H^+.

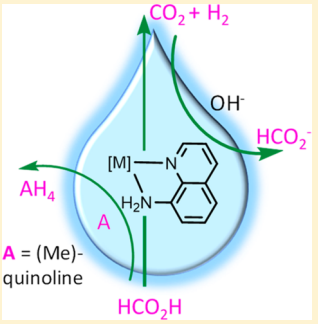

INTRODUCTION

Hydrogen-related catalytic processes are of current interest for the scientific community, not only due to their numerous practical applications,[1] but also for the intriguing characteristics of the transition metal hydrides and dihydrogen complexes.[2] In this context, one motivating and current challenge related to sustainability is the catalytic CO_2 hydrogenation[3,4] to one-carbon molecules such as formic acid[4] (or formate)[5] or methanol as an alternative to photo-[6] and electrochemical[7,8] CO_2 reduction. The interest in formic acid in relation to CO_2 conversion derives from the fact that it is the liquid product of CO_2 hydrogenation that requires the lowest consumption of H_2.[9] Formic acid can be used as a feedstock in chemical reactions but it can also be employed in fuel cells.

In addition to the above, hydrogen has been postulated as an alternative energy source for future generations due to its high gravimetric energy density and its environmental advantages (water is the only byproduct).[10] The manipulation, storage, and transport of molecular hydrogen is dangerous and very inefficient. As a consequence, the development of hydrogen storage systems is highly desired.[11,12] Formic acid (FA) is considered a leading system for hydrogen storage,[4,11,13] because it combines a moderately high H_2 content (4.38 wt %, 53 $g \cdot L^{-1}$) with a number of advantageous properties related to its safe transportation and manipulation.[14,15] Interestingly, FA is a major product of biomass processing.[13]

Different complexes of Ru, Rh, Ir, and Fe, mainly with P- or N-donor ligands including half-sandwich derivatives and others that contain pincer ligands (usually of the PNP type), have been reported as precatalysts in the FA dehydrogenation.[13,14,16−26] Catalytic hydrogenation of CO_2 has been reported most frequently for ruthenium complexes but iridium, rhodium, iron, cobalt, nickel, copper, manganese, and molybdenum derivatives have also been described.[4,5,14,27−32]

Received: July 31, 2018

DOI: 10.1021/acs.inorgchem.8b02164
Inorg. Chem. XXXX, XXX, XXX−XXX

The concept of TH of CO_2 to formate was first proposed by Peris in 2010.[33] High activities have been attained in the hydrogenation of bicarbonate with half-sandwich Rh, Ir, or Ru with dihydroxy-phenanthroline ligands (proton-responsive ligands) although the use of high pressures is required (about 40 bar).[34,35] In general, harsh conditions of temperature and pressure are commonly required for such processes.[14,32] Although examples with low temperatures have been reported (50−80 °C), the use of 100−200 °C is rather common and pressures clearly higher than 25−25 (CO_2/H_2) bar are generally used. Systems that are active in both transformations have been reported,[36,37] and a detailed review about noble and non-noble metal based catalysts for both processes has been recently published.[14] One again, high pressures for the CO_2 hydrogenation,[35,37−41] high catalyst loadings,[42] and/or the use of organic solvents are usually needed.[40,41,43] Fukuzumi et al. described a process that takes place at atmospheric pressure, although this requires a high catalyst concentration and provides a low TON (100).[44] As a consequence, the development of new, facile, efficient, and robust versatile catalysts for both processes that work in water, as a benign solvent, and under mild conditions is highly desirable.

The metal-catalyzed generation of H_2 from FA is closely related to the use of this acid (in a buffer with formate) as a hydrogen donor for transfer hydrogenation (TH) reactions in water.[45−48] TH has been frequently used for the hydrogenation of carbonyl compounds[46,49] and imines,[50] but the hydrogenation of heteroaromatics is more challenging.[51] The selective hydrogenation[51−53] of the pyridinic ring of quinolines leads to 1,2,3,4-tetrahydroquinolines, which are important synthetic intermediates for pharmaceuticals, agrochemicals, and dyes.[54,55] Examples of this hydrogenation with the FA/formate mixture in water with Ir, Rh, and Ru complexes have appeared in the bibliography.[56−58] Xiao[59] reported the use of Ir complexes with low catalyst loadings, and interesting mechanistic studies were also described. The handling of molecular hydrogen to reduce these substrates is less convenient and, with some exceptions,[60] either high pressures[61−67] or high temperatures[68] are required. It is generally accepted that an ionic mechanism occurs that involves hydride transfer to a previously protonated form[58−60] of the quinoline derivative. Moreover, a clear effect of the pH of the medium has been observed and acidic values (4.5−5) are needed for an optimal reduction.

The importance of secondary coordination sphere interactions on using multifunctional ligands[69] has been documented in different fields including H_2 production and CO_2 reduction.[70] For example, in complexes with pincer ligands the formation of a hydrogen bond with the ligand allows the insertion of CO_2 into an Ir−H bond in a very active system[71] and cases of ligand-assisted H_2 activation have been reported.[27,36] Long-range metal−ligand bifunctional catalysis involving FA-assisted proton hoping in a dehydrogenation process of this acid has also been described.[72]

We describe here a series of half-sandwich Ru, Ir, and Rh complexes with κ^2-*N*,*N*′-chelating ligands, which could participate actively in the catalytic process. The ligands chosen (see Chart 1) contain one or more $-NH_2$ groups that are able to form hydrogen bonds in all cases but would be arranged at different distances from the metal center. Interestingly, it was found that one Rh complex and another Ir derivative are versatile catalysts that are active in (i) CO_2 hydrogenation, (ii) dehydrogenation of formic acid into H_2 and CO_2, and (iii) selective TH of quinolines with HCO_2H/HCO_2Na as the hydrogen source in water.

Chart 1

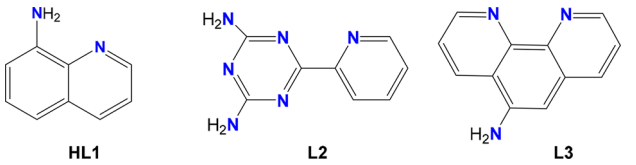

We also report on the detection and study of the possible intermediates in the catalytic processes and the behavior in D_2O of the metal hydrides by analyzing the presence or absence of an umpolung process (i.e., reversal of polarity, transformation of D^+ into M−D). An interchange between a hydrido and an amido iridium species derived from ligand HL1 was identified. The formation of HD or D_2 with D_2O as the only deuterium source has also been considered. The results reported here could open new ways for the design of improved catalytic systems.

RESULTS AND DISCUSSION

Synthesis of Complexes. The structural formulas of the complexes reported in this work are provided in Scheme 1. The cationic *p*-cymene complex $[(\eta^6\text{-}p\text{-cym})RuCl(HL1)]Cl$, **I**, was prepared by reacting the dimer $[(\eta^6\text{-}p\text{-cym})Ru(\mu\text{-}Cl)Cl]_2$ with 8-aminoquinoline (HL1) at room temperature. Treatment of complex **I** with $NaBF_4$ afforded **1BF$_4$**. The change in the anion was performed in order to obtain a compound that could give rise to single crystals appropriate for an X-ray diffraction study. The neutral complex **2** was prepared adding KOH after the reaction of the dimer and the ligand. Pentamethylcyclopentadienyl (Cp*) cationic complexes of stoichiometry $[(\eta^5\text{-Cp}^*)M(N,N')]Cl$, **3** to **7**, were prepared by treating the appropriate dichloro-bridged dimer $[(\eta^5\text{-Cp}^*)M(\mu\text{-}Cl)Cl]_2$ (M = Rh, Ir) with the corresponding ligand. Complex **I** has been reported by Türkmen et al. and Singh et al. independently,[73,74] but it was synthesized in this work for the sake of comparison in the catalytic tests.

Characterization by NMR Spectroscopy. The ^1H NMR and $^{13}C\{^1H\}$NMR spectra are consistent with the structural formulas depicted in Scheme 1. 2D NMR spectra and NOE effects were used to assign the resonances (see Figure S1 for the NOE effects in **2**). The Ru(II) *p*-cymene complexes **I**, **1BF$_4$**, and **2** showed patterns consistent with a C_1 symmetry.

The 2D NOESY spectrum registered for **I** exhibits exchange cross-peaks between the pairs H^2−H^6, H^3−H^5, and H^8−H^9, which evidence a dynamic process that allows interconversion between enantiomers R_{Ru} and S_{Ru}.

The resonances of the $-NH_2$ groups deserve further comment: Complexes **I**, **3**, and **4**, with 8-aminoquinoline, display two resonances at very different chemical shifts (for instance, δ 11.72 and 4.61 ppm, $^2J_{HH}$ = 10.55 Hz for **I**) and these signals are attributed to inequivalent protons of this group. This observation is consistent with an *N*,*N*′ chelate coordination mode for HL1 and suggests that the −NH proton at lower field is involved in a hydrogen bonding interaction, possibly with the chloride ligand. Moreover, it was confirmed that these protons do not exchange with one another on the NMR time scale. In the case of **7**, which contains ligand L3 where the amino group is not coordinated, a unique and broad resonance was observed for the $-NH_2$ group. The NH group

DOI: 10.1021/acs.inorgchem.8b02164
Inorg. Chem. XXXX, XXX, XXX−XXX

Scheme 1. Synthesis and Molecular Structure with Atomic Numbering of the Complexes Described in This Paper[a]

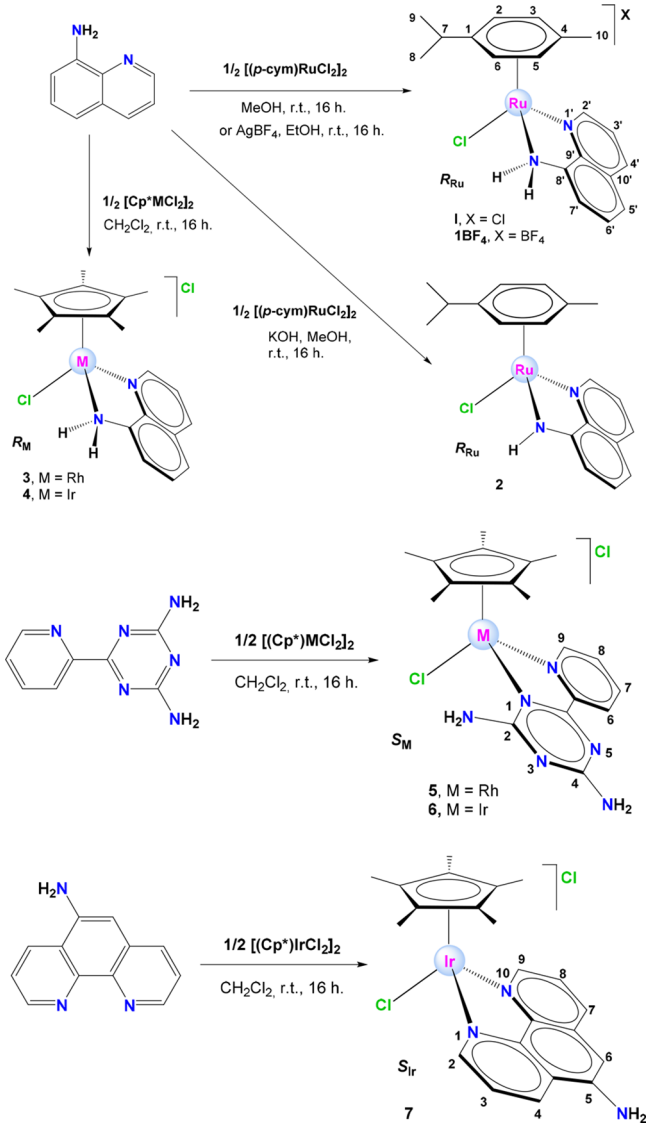

[a]Only one enantiomer is shown.

of **2** gives rise to a singlet at 8.17 ppm integrating for 1H. Besides, the neutral nature of this compound leads to a shifting to higher field of the resonances of the L1 ligand as compared to **I**.

Solid-State Characterization of $1BF_4$. The molecular and crystal structure of complex $\mathbf{1BF_4}$ was solved by X-ray diffraction. The crystallographic data and the distances and bond angles are gathered in the Supporting Information (Tables S1 and S2). An ORTEP of the cation is included in Figure 1. Both enantiomers (R_{Ru} and S_{Ru}) are present in the crystal. As **I** or the similar complex with benzene, previously described,[74] $\mathbf{1BF_4}$ has a three-legged piano-stool structure formed by the η^6-coordinated *p*-cymene ring, the (κ^2-*N*,*N*′) chelate HL1 and the chloride ligand. The 8-aminoquinoline ligand is essentially planar. The value of the bite angle is 78.70(9)°, similar to **I**.[74] The bond lengths within the cationic Ru-centered component are in the expected range[75−78] and these include the Ru−$C_{p\text{-cymene}}$ average distance of 2.19 Å. When compared with **I** the bonds involving the Ru atom are

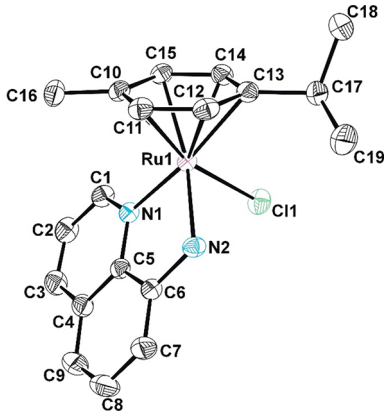

Figure 1. ORTEP of the cation in complex $\mathbf{1BF_4}$. H atoms have been omitted for clarity. Ellipsoids are shown at the 30% probability level. Selected distances (Å): Ru1−Cl1 = 2.3984(8); Ru1−N1 = 2.100(2); Ru1−N2 = 2.128(2); Ru1−$C_{average}$ = 2.19; Ru1−Centroid(p-cym) = 1.43. Bite angle N1−Ru1−N2 = 78.70(9)°.

similar except the Ru−NH_2 distance that is shorter for $\mathbf{1BF_4}$ (2.128(2) and 2.134 for **I**).[74] Interestingly, the N−H bond distances are longer in $\mathbf{1BF_4}$ (0.97 Å) than in **I** (0.91−0.92 Å).[74] The shortening of the Ru−NH_2 distance implies a higher electron donation from the N atom increasing the positive charge of this atom and this causes a lengthening of the N−H distances.

The 3D structure is held together by a set of intermolecular interactions. The chloride ligand and the tetrafluoroborate anion connect three or four, respectively, cations through hydrogen bonds, including bifurcated and trifurcated bonds. The hydrogen atoms that participate in these bonds are not only those of the −NH_2 group (interacting with the BF_4^- anion or the chloride ligand) but also H−C(sp^2) and H−C(sp^3) atoms (see Table S3). A $\pi-\pi$ interaction[54] is also established between two cations and this involves the aromatic rings that bear the amino group (see Figure S2 and Table S4).

Catalytic Transfer Hydrogenation of Quinolines. It was decided to study the catalytic activity of the complexes in the transfer hydrogenation (TH) of quinoline and methyl- and amino-substituted quinolines using HCO_2H/HCO_2Na as the hydrogen source in water. Based on literature reports[59] and on our previous results on the TH of ketones with the same hydrogen source, we chose to perform all the tests at pH 4.5.

2-Methylquinoline (**IIa**) was quantitatively reduced to 2-methyl-1,2,3,4-tetrahydroquinoline, **IIb**, within 24 h at room temperature using a 0.1 mol % loading of **3** or **4** (Table 1, entries 3 and 6). The same result was obtained on using a mixture of $[Cp^*IrCl_2]_2$ and 8-aminoquinoline, HL1, (Table 1, entry 12). However, on using only the iridium dimer, $[Cp^*IrCl_2]_2$, the yield decreased to 50% and activity was not observed with HL1 in the absence of any metallic center (entries 13 and 14). The performance of **I**, **6**, and **7** was disappointing (<1% yield after 24 h, entries 1, 10, and 11) while the activity of **5** was only moderate (entry 9). Although the activity of the Ru dimer, $[(p\text{-cym})RuCl_2]_2$, was low (entry 15), it was higher than that of the preformed complex **I**. As a control experiment, it was verified that the TH of **IIa** did not take place in the absence of any precatalyst (entry 16).

Interestingly, the application of the aforementioned TH conditions to quinoline (**IIIa**) using **4** as the precatalyst led to the hydrogenation of the pyridinic ring along with the introduction of a formyl group on the nitrogen atom in a

DOI: 10.1021/acs.inorgchem.8b02164
Inorg. Chem. XXXX, XXX, XXX−XXX

Table 1. TH of 2-Methylquinoline (IIa) and Quinoline (IIIa) Using Different Precatalysts[a]

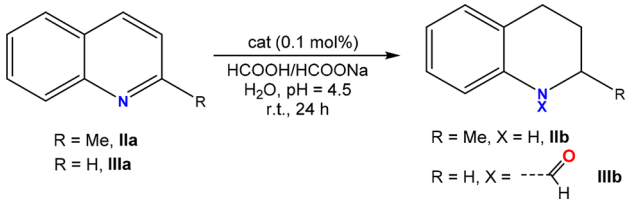

Entry	Substrate	Cat	Time (h)	Yield (%)	TON (TOF, h^{-1})[b]
1	IIa	I	24	0	--
2	IIa	2	24	0	--
3	IIa	3	24	>99	990
4	IIa	3	3	8	80
5	IIa	3	1	2	20 (20)
6	IIa	4	24	>99	990
7	IIa	4	3	13	130
8	IIa	4	1	6	60 (60)
9	IIa	5	24	40	400
10	IIa	6	24	1	10
11	IIa	7	24	1	10
12	IIa	$[Cp^*IrCl_2]_2$ + HL1	24	>99	990
13	IIa	$[Cp^*IrCl_2]_2$	24	50	500
14	IIa	HL1	24	0	--
15	IIa	$[(p\text{-cym})RuCl_2]_2$	24	20	200
16	IIa	No	24	0	--
17	IIIa	4	24	33	333

[a]Reaction conditions: 0.1 mol % of catalyst (0.09 mol % in the case of 7). Substrate: 2.5 mmol. Reaction in water with HCO_2H/HCO_2Na (pH = 4.5) in 3 mL of H_2O at r.t. [b]Calculated at 1 h.

one-pot reaction (**IIIb**, Table 1). The product was obtained in moderate yield (Table 1, entry 17). The lower yield with respect to the hydrogenation of **IIa** could be related to a lower degree of protonation of **IIIa** (pK_a(**IIIa**) = 4.94 and pK_a(**IIa**) = 5.83). The reactivity of the formyl group introduced in **IIIb** opens new reaction pathways for 1,2,3,4-tetrahydroquinoline derivatives. The formylation of 1,2,3,4-tetrahydroquinolines with different reagents has been described previously,[79−83] usually through heterogeneous catalysts, but the two-step one-pot process starting from quinoline is usually nonselective[84] and/or requires high temperatures (sometimes the reaction is also carried out under pressure).[85−88] A case with selectivity toward one of the two hydrogenated products (formylated and nonformylated) thanks to pH changes with a silica-supported iridium catalyst has recently been reported (80 °C).[88]

Catalytic tests were also performed to hydrogenate 8-aminoquinoline (**IVa**) with **3**−**7**. In these cases hydrogenation was observed in a very small extent (<5%) under the conditions explored. However, the product corresponding to the formylation of the amino group was the main product (Table 2). The hydrogenation of **IVa** was attempted again using **4** as the precatalyst at a lower pH (3.2) in an effort to improve the protonation of 8-aminoquinoline. Although formylation was observed, the hydrogenation was not improved. It is noteworthy that **7**, a precatalyst that is practically inactive in the hydrogenation of 2-methylquinoline (**IIa**), gave the best result in this process with a yield of 96%. When the activity of **4** or **7** is compared with that of mixtures of $[Cp^*IrCl_2]_2$ and the corresponding ligands (HL1 or HL3, respectively), a decrease in the activity is observed, especially

Table 2. Results Obtained in the TH of 8-Aminoquinoline Using Different Precatalysts[a]

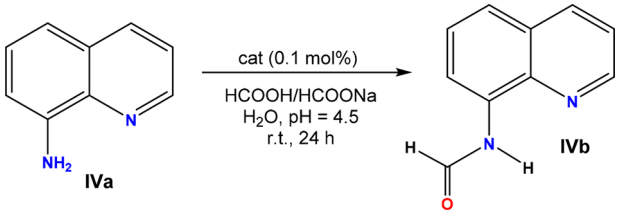

Entry	Cat	Time (h)	Yield (%)	TON (TOF, h^{-1})[b]
1	3	24	60	600
2	4	24	74	740
3	$[Cp^*IrCl_2]_2$ + HL1	24	37	370
4	4	1	19	190 (190)
5	5	24	42	422
6	6	24	27	270
7	7	24	96	961
8	$[Cp^*IrCl_2]_2$ + HL3	24	72	620
9	7	1	33	330 (330)
10	No	24	0	--

[a]Reaction conditions: 0.1 mol % of catalyst (0.09 mol % in the case of 7). Substrate: 2.5 mmol. Reaction in water with HCO_2H/HCO_2Na (pH = 4.5) in 3 mL of H_2O at r. t. during 24 h. The amount of hydrogenated product was lower than 5%. [b]Calculated at 1 h.

in the case of **4** (compare entry 2 vs 3 and entry 7 vs 8). Moreover, it was verified that a precatalyst was necessary for the process to occur, thus reflecting the formylation catalytic activity of these complexes. The generation of formamides by reaction with FA is a process that requires high temperatures and these are clearly higher than those required for the generation of acetamides, for example. In our examples, however, the process takes place at room temperature. The reported formylation of 8-aminoquinoline requires the use of toluene at reflux.[89] Hydrogenation of 8-aminoquinoline has been reported but higher temperatures are required (toluene at reflux).[90]

The three quinolines tested in the catalytic experiments are not soluble in the solutions in the catalytic conditions. Thus, the processes are biphasic in nature.

Some cases have been reported of the dehydrogenation of 1,2,3,4-tetrahydroquinolines.[91,92] Catalytic tests were performed with **4** and 1,2,3,4-tetrahydroquinoline (0.1% mol and 1% mol) or with 2-methyl-1,2,3,4-tetrahydroquinoline with the same precatalyst (0.1% mol) at 80 °C in 2,2,2-trifluoroethanol during 20 h. However, the amounts of the dehydrogenated products, quinoline and 2-methylquinoline, were very small (yield <1%).

Catalytic Dehydrogenation of Formic Acid. Complexes **I** and **3**−**7** were tested as potential catalysts for the dehydrogenation of a mixture of formic acid/sodium formate at 100 °C and pH 4.5, using 0.04 mol % of the respective precatalysts. The gas formed was collected with a gas buret. It was verified that a certain amount of CO_2 was present in the gas mixture on using a buret filled with water (as verified by bubbling the gas through CD_3CN, signal at 125.5 ppm in the $^{13}C\{^1H\}$ NMR spectrum). As a consequence, the buret was filled with aqueous NaOH solution (0.1 M). In this case, CO_2 was not detected in the gas mixture collected. The amount of H_2 generated by **I** and **5**−**7** was very small. However, **3** and **4** were active in this process (see Table 3). In the initial period of the reaction (5−10 min), **3** provided better performance than

DOI: 10.1021/acs.inorgchem.8b02164
Inorg. Chem. XXXX, XXX, XXX−XXX

Table 3. Dehydrogenation of Formic Acid Catalyzed by the Indicated Complexes[a]

Entry	Cat	time (min)	V(H_2)[b], L	n(H_2), mol	TON (TOF, h^{-1})[c]
1	I	120	0	0	--
2	3	5	0.290	1.18×10^{-2}	641
3	3	10	0.400	1.63×10^{-2}	886
4	3	21	0.490	2.00×10^{-2}	1087
5	3	50	0.640	2.61×10^{-2}	1418
6	3	60	0.690	2.87×10^{-2}	1560 (1560)
7	3	120	0.855	3.56×10^{-2}	1935
8	3	180	0.950	3.88×10^{-2}	2109
9	4	5	0.200	8.16×10^{-3}	443
10	4	10	0.360	1.47×10^{-2}	799
11	4	21	0.685	2.80×10^{-2}	1522
12	4	50	1.160	4.74×10^{-2}	2576
13	4	60	1.250	5.20×10^{-2}	2826 (2826)
14	4	120	1.345	5.60×10^{-2}	3043
15	4	200	1.400	5.72×10^{-2}	3109
16	5	120	0	0	--
17	6	120	0	0	--
18	7	120	0	0	--

[a]The reaction was performed using a mixture of HCO_2H/HCO_2Na (0.05:0.105 mol) in 10 mL of H_2O in the presence of the corresponding catalyst (1.84×10^{-5} mol, 0.04 mol %) at initial pH 4.5 and 100 °C. [b]Yield of H_2 gas collected in a gas buret filled with a 0.1 M NaOH solution. [c]Calculated at 60 min.

4 (cf. entries 2 vs 9 and 3 vs 10) whereas after approximately 21 min **4** provided a better TON value than **3** (entries 4 and 11) (see Figure S3).

The most active systems reported until now include complex **A** of Chart 2 (3.1 μM, 90 °C, TON = 165×10^3 after 7 h, TOF(h^{-1}) = 228×10^3),[35] the Ru derivative [RuHCl(CO)-(^{t}Bu$_2$PCH$_2$NC$_5$H$_3$CH$_2$P^{t}Bu$_2$)] (1.42 μM, 90 °C, TON = 706.5×10^3 after 3 or 4 h, TOF(h^{-1}) = 256×10^3)[43] and the Fe complex [FeH(HCO$_2$)(CO)(^{i}Pr$_2$P(CH$_2$)$_2$NH(CH$_2$)$_2$P^{i}Pr$_2$)] (0.0001 mol % cat, 10 mol % $LiBF_4$, 80 °C, TON = 983,642 in 9.5 h, TOF(h^{-1}) = 196,728).[18] However, although complex **A** was used in aqueous solutions, the FA decomposition with the Ru and Fe complexes was carried out in organic solvents as DMF and dioxane, respectively.

Chart 2

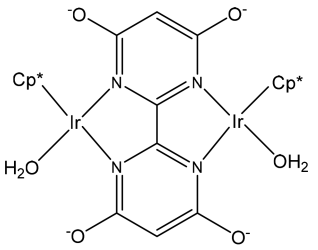

A

In the case of **4**, further experiments were carried out to obtain information about the possible mechanism of the process: (i) the initial rates of decomposition of the mixture HCO_2H/HCO_2Na in catalytic experiments with H_2O and D_2O were compared and an isotopic effect of 1.41 was observed ($r(H_2O)/r(D_2O)$ = 1.41; see Figures S4 and S5); (ii) analysis of the gas evolved in a catalytic process performed in D_2O showed the presence of H_2, HD, and D_2. ^{1}H NMR spectroscopy allowed H_2 and HD to be detected in a H_2:HD ratio of 20:80 (see Figure S6). A ^{2}D NMR spectrum allowed the detection of D_2 but the amount of HD was not sufficiently high to be observed in this spectrum (see Figure S7). Thus, the three possible isotopomers of molecular hydrogen were detected in the following sequence of increasing concentration: $H_2 < HD \ll D_2$.

As for **3**, in the catalytic dehydrogenation experiment with the HCO_2H/HCO_2Na mixture in D_2O, both H_2 and HD were detected in a H_2:HD ratio of 26:74 but in this case the formation of D_2 was not observed.

CO_2 Hydrogenation. Complexes **I** and **3**−**6** were tested as precatalysts in the hydrogenation of CO_2 using pressures of 5 bar of H_2 and 5 bar of CO_2 in 0.1 M aqueous KOH at 80 °C during 8 h. The results are gathered in Table 4. Potassium

Table 4. Hydrogenation of CO_2 Catalyzed by the Complexes Indicated[a]

Entry	Precatalyst	Time (h)	T (°C)	HCO_2K generated (mol)	TON
1	I	8	80	0.00139	5562
2	I	3	40	nd	--
3	3	8	80	0.00150	5991
4	3	3	40	nd	--
5	4	8	80	0.00151	6021
6	4	3	40	0.00142	5662
7	5	8	80	nd	--
8	6	8	80	nd	--

[a]Precatalyst = 50 μM. 5 mL of a 0.1 M KOH solution in H_2O. P(H_2) = 5 bar, P(CO_2) = 5 bar.

formate was only generated in the case of complexes **I**, **3**, and **4**. When the temperature and the time were reduced to 40 °C and 3 h, respectively, the potassium salt was not detected in the case of **I** and **3**, but the number of moles were only slightly reduced in the case of **4**, which was the most active precatalyst (see Figures S8−S10 and Table S5 for more information about the experimental procedure).

Some very active systems previously described include iridium catalysts as [IrH_3(^{i}Pr$_2$PCH$_2$NC$_5$H$_3$CH$_2$P^{i}Pr$_2$)] (200 °C, 50 bar, 0.010 μM, 300×10^3 TON, 150×10^3 TOF, h^{-1}),[28] complex **A** of Chart 2 (80 °C, 50 bar, 2 μM, 79×10^3 TON, 53.8×10^3 TOF h^{-1})[35] or the Ru derivative [RuHCl(CO)(^{t}Bu$_2$PCH$_2$NC$_5$H$_3$CH$_2$P^{t}Bu$_2$)] (120 °C, 40 bar, 0.178 μM, 1100×10^3 TOF h^{-1}).[43] However, this last catalytic process was performed in DMF. The two last ones were also very active on FA decomposition. To the best of our knowledge, the lowest total pressure reported (10 bar, 50 μM), similar to our examples, is reported with complex **A** and gives rise to a TON value of 7200 but after 336 h (64 TOF h^{-1}). Thus, our results are outstanding because of the low pressure used (10 bar, 5662 TON at 3 h with **4**).

From the different catalytic studies performed it is observed that apparently the NH_2 group of HL1 exerts a positive effect as it has also been recently reported in other types of Ir complexes with this ligand.[22]

Mechanistic Studies. Characterization of Catalytic Intermediates. Some experiments were performed to get information about the possible catalytic intermediates in the FA decomposition process or to find out the role of the $-NH_2$ group of the HL1 ligand. The ^{1}H NMR spectra in D_2O at 25 °C of complexes **I**, **3**, **4**, and **6** were recorded, and after that,

DOI: 10.1021/acs.inorgchem.8b02164
Inorg. Chem. XXXX, XXX, XXX−XXX

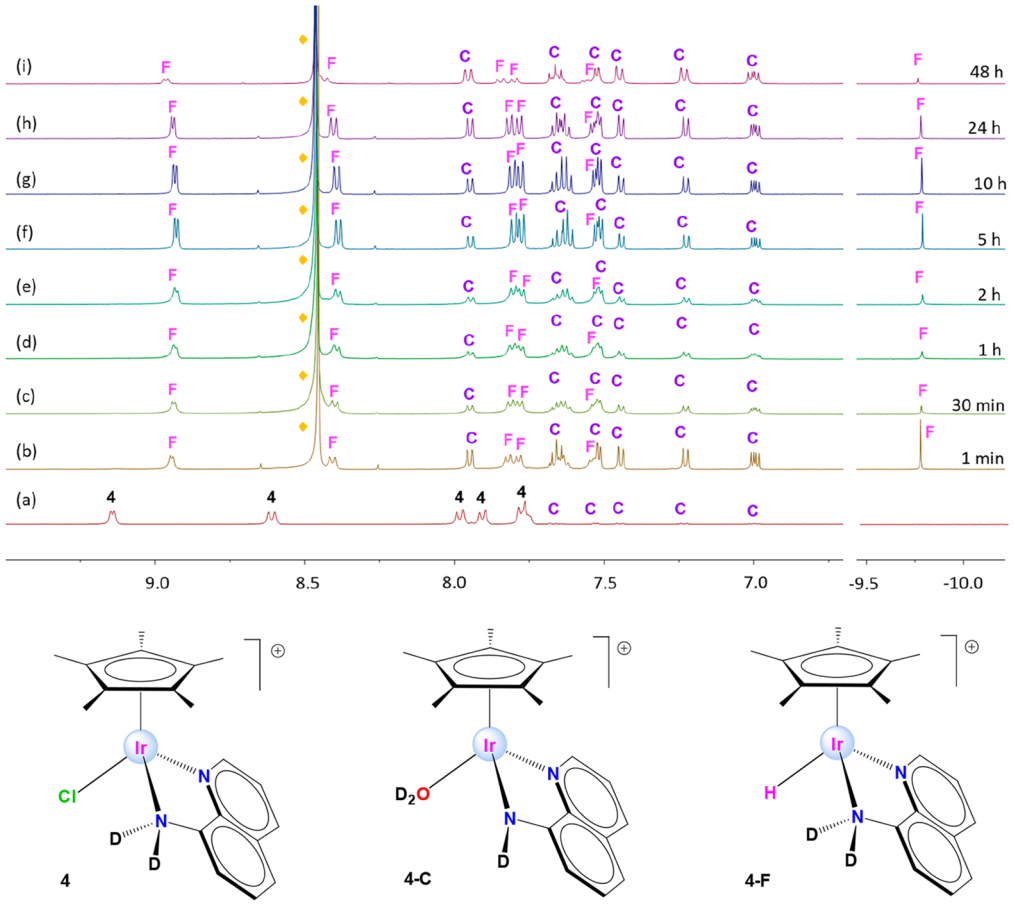

Figure 2. Aromatic region (left) and hydride region (right) of ^{1}H NMR spectra of (a) Complex **4** in D_2O (7.5×10^{-3} mmol) at 25 °C. The species **4** $[Cp^*IrCl(HL1)]^+$, coexist with a small amount of **4-C** (**C**) $[Cp^*Ir(D_2O)(L1)]^+$. (b–j) Spectra corresponding to the evolution with time of the solution of 'a' after adding HCO_2Na (6.5×10^{-2} mmol). **4-C** and **4-F** (**F**) $[Cp^*IrH(HL1)]^+$ coexist. Free formate is labeled as yellow ♦).

the evolution with time under pseudocatalytic conditions, i.e., in the presence of an excess of HCO_2Na (1:9 molar ratio) in D_2O was monitored. At room temperature and at the moderately alkaline pH (8.29) of these experiments we anticipated that the FA decomposition reaction could be slowed down and that catalytic intermediates could be detected.

The spectra of **4** in neat D_2O displayed two sets of signals for two products in an approximate 9:1 ratio (Figure 2(a)). The major component is tentatively attributed to the chlorido-precatalyst while the minor component is assigned as a new derivative (labeled as **4-C**) (see Scheme 2 for the labeling of the intermediates). Several additional NMR experiments were carried out to establish the identity of **4-C**: (i) Na_2CO_3 was added to **4** in D_2O and this resulted in the quantitative formation of **4-C** (see Figure S11). (ii) DCl (1 M in D_2O, 50 μL) was added to **4-C** and resonances with δ values consistent with **4** emerged (see Figure S11). All of these results prove that the formation of **4-C** from **4** involves a deprotonation process. However, inasmuch as species **4** and **4-C** can be distinguished by NMR, we believe that the transformation of **4** into **4-C** must involve a second process, such as aquation (Ir–Cl → Ir–OH_2 exchange). Hence, we propose that the minor intermediate **4-C** could well be formulated as two species in fast equilibrium: (i) the aqua-amido complex **4-C1** of formula $[Cp^*Ir(D_2O)(L1)]^+$ (see Scheme 2) where the $-ND_2$ group of HL1 has been converted into an amido group –ND and (ii) the corresponding hydroxo-amino complex, $[Cp^*Ir(OD)(HL1)]^+$ (labeled as **4-C2**, see Scheme 2). From now on, we will use the symbol **C** when referring to the two species **C1**/**C2** in equilibrium.

In the first spectrum recorded after the addition of HCO_2Na to the solution of **4** in D_2O (see spectrum (b) in Figure 2 and S12) the signals attributed to **4** vanished and a sharp increase in the peaks assigned to **4-C** was observed along with the appearance of resonances for a hydrido-derivative, Ir–H (**4-F**). The latter assignment was made on the basis of the signal observed at −9.78 ppm (see Figure 2). The formation of monohydrides from the reaction of half-sandwich complexes of late-transition metals in the presence of HCO_2Na is well-documented.[93] Interestingly, during the first 48 h a fluctuation was observed in the integration ratio between signals of **4-C** and **4-F** together with a slow release of bubbles (presumably H_2 + CO_2). However, after this time the evolution of gas had stopped and the concentration of hydride **4-F** had diminished considerably. This finding is consistent with the arrest of the catalytic decomposition of FA due to the expected increase in pH even though the HCO_2Na had not been completely consumed.

A comparative analysis of the integrals for the hydride resonance of **4-F** and that for the signal at 8.95 ppm belonging to the same species reveals a partial deuteration of the Ir–H group and accordingly, the Ir–D group was detected by ^{2}D NMR spectroscopy (resonance at −9.71 ppm, see Figure

DOI: 10.1021/acs.inorgchem.8b02164
Inorg. Chem. XXXX, XXX, XXX–XXX

Scheme 2. Cycle Proposed for the Evolution of a Solution of 4 with HCO_2Na in D_2O

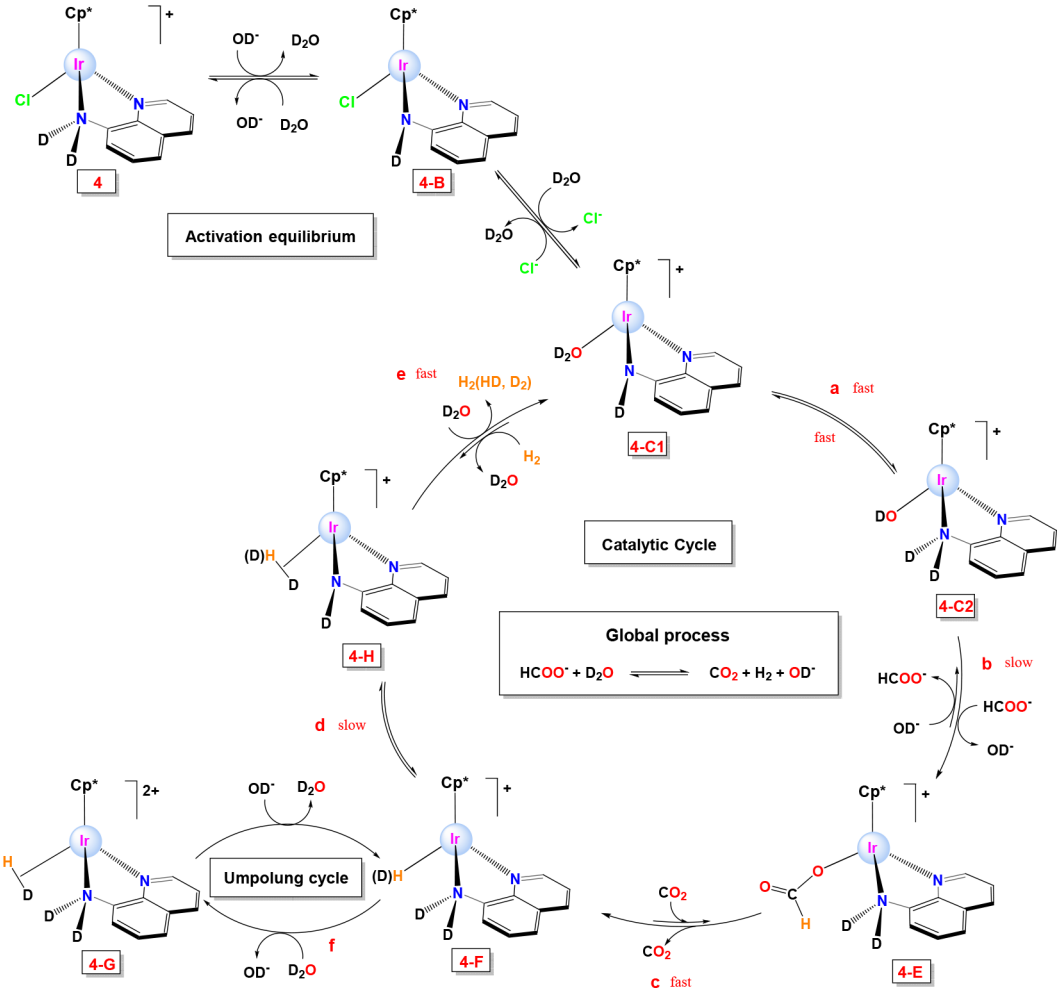

S13).The variation of the Z value (see eq 1) is represented in Figure S14. The initial value of 0.72 decreased sharply in the first hour and then diminished more slowly up to 5 h before a value between 0.3−0.4 was reached up to 25 h. After 11 days the value of Z was 0.25.

$$Z = \frac{(\mathrm{Ir} - \mathrm{H})}{(\mathrm{Ir} - \mathrm{H}) + (\mathrm{Ir} - \mathrm{D})} \quad (1)$$

Ir−H = integral of the hydride resonance of **4-F** in the ^{1}H NMR spectrum.

(Ir−H) + (Ir−D) = integral of the resonance at 8.95 ppm of **4-F** in the ^{1}H NMR spectrum.

From the results described above it can be concluded that (a) complex **4** can promote the catalytic release of CO_2 and H_2 even under adverse conditions (alkaline pH, 8.29); (b) the chloro-amino species **4** is only the precatalyst and it does not take part in the catalytic cycle; (c) the species **4-C** and **4-F** are active intermediates in this process and can be considered as resting states of the catalytic cycle; (d) the hydrido species **4-F** undergoes partial deuteration, thus suggesting its participation in an umpolung process (*vide infra*).

The mechanism proposed for the decomposition of HCO_2Na in the presence of **4** is outlined in Scheme 2. The process consists of two consecutive activation steps and a catalytic cycle in which only the species **4-C** and **4-F** have been detected experimentally. We theorize that in the presence of formate the activation steps are shifted toward the production of **4-C1** from **4**. Then, the cycle starts with an equilibrium between **4-C1** and **4-C2**. In step b, **4-C2** undergoes a substitution reaction to give the formate complex, **4-E**. This step must be rate-determining in agreement with the observation of **4-C**. Complex **4-E** rapidly evolves to the hydride derivative **4-F**. Indeed, the absence of signals for the species **4-E** and the observation of resonances for the hydrido intermediate **4-F** in this ^{1}H NMR study indicates that step **c** is fast and that step **d** is rate limiting. This fact is in accordance with the isotopic effect observed when using D_2O instead of H_2O always in the presence of HCO_2H (*vide supra*). The species **4-F** undergoes an [Ir]−H ↔ [Ir]−D exchange by an umpolung process (reversal of polarity, in this case D^+ from water $D(\delta^+)$-OD is transformed into $Ir-D(\delta^-)$). The occurrence of the umpolung process is deduced both from the reduced integral area of the Ir−H resonance and from the formation of D_2 in the catalytic process. The umpolung process may take place, as observed in other examples[93−95] by reaction of D^+ with the Ir−H group and formation of $[Cp^*Ir(HD)(HL1)]^{2+}$ (**4-G**) provided that step **d** is slower than step **f**. In this part of Scheme 2, deuterium atoms, D, are shown in brackets to reflect the possible incorporation of deuterium in the cycle. Next, it is postulated that an internal deuterium transfer process slowly converts **4-F** into the undetected intermediate **4-H** (step **d**). Finally, the cycle is closed through

DOI: 10.1021/acs.inorgchem.8b02164
Inorg. Chem. XXXX, XXX, XXX−XXX

the fast release of hydrogen (step **e**) and the regeneration of **4-C1**.

In order to obtain more information to support our proposal, the effect of the addition of HCl (HCl:**4** ratio of 2) to the sample after 11 days, which contained mainly **4-C** and 6% of **4-F** with $Z = 0.25$, was analyzed. The release of gas was observed and after 5 h 61% of **4-F** was present and the Z value was 0.13. These facts indicate, as proposed, that the acidic medium favors the formation of **4-F** from **4-C** because the rate limiting step **b** is promoted by a decrease in the OD^- concentration and this allows the catalytic cycle to restart. Moreover, this situation also favors the deuteration of the Ir−H group thanks to the promotion of step **f**. Four days after the addition of the acid the major product was **4-C** and the percentage of **4-F** was 12%. At this point, the amount of formate had been markedly reduced to an HCO_2^-:(**4-C**+**4-F**) ratio of 0.2. The value of Z at this point was 0.06 and this shows a high degree of deuteration.

Considering all the information discussed above, we propose that the catalytic hydrogenation of CO_2 ($P(CO_2) = P(H_2) = 5$ bar) in the presence of **4** at basic pH must proceed by a pathway opposite to that depicted in Scheme 2 (i.e., in an anticlockwise sense). Thus, we believe that **4-C1** is able to coordinate a molecule of H_2 to give intermediate **4-H**, which in turn can heterolytically activate this molecule to give **4-F**. CO_2 is then inserted into the Ir−H bond to produce **4-E**, so that in the next step the anion formate is eliminated to generate **4-C2**, which is in equilibrium with **4-C1**. However, for the dehydrogenation of the mixture HCO_2H/HCO_2^-, which has been studied at acidic pH, some species need to be reformulated (see Scheme S1). In particular, we hypothesize that the species **4-C1**/**4-C2** are not favored at acidic pH, so instead we propose that the first active species in the corresponding catalytic cycle must be the aqua-amino intermediate **4-J** ($[Cp^*Ir(DL1)(D_2O)]^{2+}$). This species can be transformed into intermediates **4-E**, **4-F**, and **4-H** under the experimental conditions to generate concurrently the gas mixture of CO_2 and H_2. It is worth noting that the **4-C1**/**4-F** couple (the same will apply for **3** and **I**; see below) could be considered as the dehydrogenated and hydrogenated forms, respectively, of a pair of species in a Noyori-type mechanism.[96]

As for **3**, the ^1H NMR in D_2O also revealed the coexistence of **3** and **3-C** (9:1 ratio, the similar nature of **3-C** and **4-C** was verified with experiments as those performed with **4-C**, Figure S15) and after the addition of 9 equiv of HCO_2Na the transformation of **3** into **3-C** takes place, with **3-C** being the only species after 72 h (see Figure S16). In this case neither the formate complex nor the hydrido-derivative were detected by NMR, which suggests that the release of both CO_2 and H_2 are fast and that **3-C** is the catalyst resting state in the HCO_2^- decomposition. In addition, the inability of **3** to produce D_2 in this reaction indicates that an umpolung process is not operating (**3-G** is not formed). The ability of Ir-Cp* complexes with bpy ligands to promote H/D umpolung processes in contrast to the inability of the analogous Rh derivatives have been reported previously.[95] Apart from the above, the cycles proposed for the FA dehydrogenation and hydrogenation of CO_2 for complex **3-A** must be similar to those depicted in Scheme 2 and Scheme S1, respectively.

The Ru complex **I** in D_2O is in equilibrium with the aqua-amino derivative, $[(p\text{-cym})Ru(HL1)(D_2O)]^{2+}$, **I-J** (Figure S17). After the addition of HCO_2Na the signals for the latter species disappeared, the intensity of the resonances of **I** decreased and two new sets of signals were observed: the formato complex (**I-E** with a coordinated formate ligand) and the aqua-amido complex (**I-C**, its nature was also verified with reactions similar to those used with **4-C**) (see Figure S18). The presence of the formato complex shows that in this case its transformation into the hydrido derivative is not a fast process. Evidence for the hydrido complex was not found and this is consistent with a fast transformation of the hydrido species into the aqua-amido derivative **I-C**.

In the case of **6**, with ligand L2, the D_2O solution only contained the initial compound and the addition of an excess of HCO_2Na initially gave rise to a mixture of three species, namely, **6**, the formate-intermediate (**6-E**) and the hydrido species (**6-F**). This mixture evolved slowly to produce the hydrido-derivative as the only species after 24 h (see Figure S19) and this exhibited remarkable stability—unlike the analogous species with ligand HL1. This difference can be explained as being the result of the position of the $-NH_2$ group in the hydrido-intermediates. In the hydrido species **4-F** (and probably in **3-F** and **I-F**), the coordinated $-NH_2$ group exhibits exacerbated acidity together with close proximity to the hydride group, in such a way that one H^+ (or D^+) is easily transferred to the hydride group to form H_2 (or HD). In other words, the ligand 8-aminoquinoline assists the metals efficiently in the HCO_2H dehydrogenation in a metal−ligand bifunctional catalysis. The fact that **6** is not active in the HCO_2H dehydrogenation regardless of the pH implies that protons are not transferred efficiently to the hydride group of species **6-F** even in the presence of HCO_2H under catalytic conditions. We also noted that for **6-F** the intensity of the hydride signal is not reduced with time with respect to other signals of the compound, thus indicating that the Ir−H ↔ Ir−D exchange does not take place.

CONCLUSIONS

Two versatile precatalysts have been synthesized, namely, $[Cp^*MCl(HL1)]Cl$ (HL1 = 8-aminoquinoline; M = Rh, **3**; Ir, **4**), and these are active in three processes that involve the concerted transfer of hydrides and protons, i.e., CO_2 hydrogenation, formic acid dehydrogenation, and transfer hydrogenation of 2-methylquinoline under mild conditions. The iridium complex **4** is more active than its relative with rhodium, **3**. The CO_2 hydrogenation takes place at a very low total pressure of 10 bar. The reaction of complexes **3** and **4** and the ruthenium derivative $[(p\text{-cym})RuCl(HL1)]Cl$ with HCO_2Na in D_2O leads to the formation of the hydrido species where the NH_2 group must be sufficiently acidic to react with the hydride. This reaction liberates XY (X or Y = H, D) and the species evolves to the amido derivative, which is detected in all cases. This evolution is only slow enough for the hydrido species to be detected in the Ir case. A pH-dependent umpolung process takes place in the iridium hydrido complex, with D^+ being transformed into Ir−D. This process also leads to the formation of D_2 as the major component of the gas in the catalytic formic acid dehydrogenation process. When the reaction with HCO_2Na is performed with the complex $[Cp^*IrCl(L2)]Cl$ (L2 = 6-pyridyl-2,4-diamine,1,3,5-triazine) the final product is the hydrido species and gas release was not observed—a finding in agreement with the lack of activity in the FA dehydrogenation. Both of these facts may be related to the absence of a coordinating $-NH_2$ group that could assist in the transfer of a proton to the Ir−H group. Thus, we can conclude that the ligand 8-aminoquinoline assists the metals

DOI: 10.1021/acs.inorgchem.8b02164
Inorg. Chem. XXXX, XXX, XXX−XXX

efficiently in the HCO_2H dehydrogenation and the coordination of the NH_2 group to the metal center imparts specific properties to the complexes, a fact that may be used in the future design of new catalytic species.

EXPERIMENTAL SECTION

General Methods and Starting Materials. The starting materials $RuCl_3 \cdot xH_2O$, $RhCl_3 \cdot xH_2O$, and $IrCl_3 \cdot xH_2O$ were purchased from Johnson Matthey and used as received. The starting dimers $[RuCl(\mu\text{-}Cl)(p\text{-cym})]_2$,[97] $[RhCl(\mu\text{-}Cl)(Cp^*)]_2$, and $[IrCl(\mu\text{-}Cl)(Cp^*)]_2$ (*p*-cym = *p*-cymene, Cp* = pentamethylcyclopentadienyl)[98,99] were prepared according to literature procedures. The ligands 8-aminoquinoline (HL1), 6-pyridyl-2,4-diamine-1,3,5-triazine (L2), and 5-aminophenanthroline (L3) were purchased from Sigma-Aldrich and were used without further purification. Deuterated solvents ($CDCl_3$, CD_3OD, and D_2O) were obtained from Euriso-top.

Synthesis Method and Complex Characterization. All synthetic manipulations were carried out under an atmosphere of dry, oxygen-free nitrogen using standard Schlenk techniques. The solvents were dried and distilled under a nitrogen atmosphere before use. Elemental analyses were performed with a Thermo Fisher Scientific EA Flash 2000 Elemental Microanalyzer. The analytical data for the new compounds were obtained from crystalline samples when possible. IR spectra were recorded on a Jasco FT/IR-4200 spectrophotometer (4000−400 cm^{-1} range) with a Single Reflection ATR Measuring Attachment. HR ESI(+) mass spectra (position of the peaks in Da) were recorded with an Agilent LC-MS system (1260 Infinity LC/6545 Q-TOF MS spectrometer) using DCM as the sample solvent and (0.1%) aqueous HCO_2H/MeOH as the mobile phase and with an autospec spectrometer. NMR samples were prepared under a nitrogen atmosphere by dissolving the appropriate amount of compound in 0.5 mL of the respective oxygen-free deuterated solvent and the spectra were recorded at 298 K on a Varian Unity Inova-400 (399.94 MHz for ^1H; 376 MHz for ^{19}F; 100.6 MHz for ^{13}C). Typically, ^1H NMR spectra were acquired with 32 scans into 32 k data points over a spectral width of 16 ppm. ^1H and $^{13}C\{^1H\}$ chemical shifts were internally referenced to TMS via the residual ^1H and ^{13}C signals of $CDCl_3$ (δ = 7.26 ppm and δ = 77.16 ppm), whereas for the ^1H NMR spectra recorded in D_2O, 1,4-dioxane (3.75 ppm) was used as internal reference according to the values reported by Fulmer et al.[100] Chemical shift values (δ) are reported in ppm and coupling constants (J) in Hertz. 2D NMR spectra such as $^1H-^1H$ gCOSY, $^1H-^1H$ NOESY, $^1H-^{13}C$ gHSQC, and $^1H-^{13}C$ gHMBC were recorded using standard pulse sequences. The probe temperature (±1 K) was controlled by a standard unit calibrated with methanol as a reference. All NMR data processing was carried out using MestReNova v 10.0.2. For the molar conductimetry measurements, the Λ_M values are given in $S \cdot cm^2 \cdot mol^{-1}$ and were obtained at room temperature for 10^{-3} M solutions of the corresponding complexes in CH_3CN, using a CRISON 522 conductimeter equipped with a CRISON 5292 platinum conductivity cell.

X-ray Crystallography. A summary of crystal data collection and refinement parameters for $\mathbf{1BF_4}$ (CCDC number 1858461) are given in Table S1. A single crystal of $\mathbf{1BF_4}$ was mounted on a glass fiber and transferred to a Bruker X8 APEX II CCD diffractometer equipped with a graphite monochromated Mo Kα radiation source (λ = 0.71073 Å). Data were integrated using SAINT[101] and an absorption correction was performed with the program SADABS.[102] The software package WINGX[103,104] was used for space group determination, structure solution and refinement by full-matrix least-squares methods based on F^2. All non-hydrogen atoms were refined with anisotropic thermal parameters and hydrogen atoms were placed using a "riding model" and included in the refinement at calculated positions.

Synthesis and Characterization of the New Complexes. See Supporting Information.

Procedure for the Catalytic Transfer Hydrogenation Experiments. Substrate (2.5 mmol) and catalyst (2.5×10^{-3} mmol) were placed in a carousel reaction tube. An aqueous solution of HCO_2H/HCO_2Na (3 mL, 14.0 mmol of HCO_2H and 29.4 mmol of HCO_2Na in 2.8 mL of H_2O, pH 4.5) was added and the mixture was stirred at 30 °C during 24 h. The reaction mixture was quenched with saturated aqueous sodium bicarbonate. The aqueous layer was extracted with ethyl acetate (3 × 10 mL) and the combined organic layers were washed with brine (20 mL). The organic layer was collected and dried over anhydrous sodium sulfate. Filtration, followed by evaporation of the solvent under reduced pressure, gave the crude reaction mixture.

Procedure for the Catalytic Dehydrogenation of HCO_2H. A stock solution of HCO_2H/HCO_2Na was prepared by dissolving HCO_2Na (71.41 g) in 19 mL of concentrated formic acid (97%) and diluting to 100 mL with distilled water.

A round-bottomed glass vessel fitted with a side arm was degassed three times and placed under an N_2 atmosphere. The HCO_2H/HCO_2Na stock solution (10 mL, pH 4.5) was added. The vessel was connected to a water-cooled condenser and this in turn to a gas collection buret (i.e., the standard water displacement apparatus to determine the volume of generated gas). The buret was charged with 0.1 M aqueous NaOH. The mixture was heated to the boiling point with stirring and allowed to reflux until pressure equilibration (i.e., until water displacement stopped in the buret). The buret was completely filled again with the NaOH solution and the precatalyst (1.84×10^{-2} mmol) was added to the vessel under N_2 flux. Volumes of collected gas were recorded periodically. The catalytic activity was calculated from the volume of displaced NaOH solution assuming that CO_2 is completely dissolved in this solution and that all the gas collected is H_2. The presence of H_2 in the collected gas was confirmed by recording a ^1H NMR spectrum of this gas dissolved in CD_3CN and the absence of CO_2 was verified by recording a $^{13}C\{^1H\}$ NMR spectrum.

Procedure to Detect the Gases in the Catalytic Dehydrogenation of HCO_2H with 4. In a 10 mL Schlenk flask, previously purged with nitrogen, complex **4** (5.3 mg, 9.31×10^{-3} mmol) was added to 5 mL of the HCO_2H/HCO_2Na stock solution. The mixture was heated under reflux for 1 h and the evolved gas was simultaneously bubbled through solutions of toluene-d_8 and toluene-H_8 in different NMR tubes. The presence of H_2 and HD in the evolved gas was confirmed by recording a ^1H NMR spectrum of the toluene-d_8 solution (20:80 ratio). In the same way, the presence of D_2 was confirmed in the toluene-H_8 solution.

Procedure to Detect the Gases in the Catalytic Dehydrogenation of HCO_2H with 3. This was carried out in a similar way to that performed with **4**. In this case, 4.4 mg (8.99×10^{-3} mmol) of **3** were used. The presence of H_2 and HD in the evolved gas was confirmed by recording a ^1H NMR spectrum of this gas dissolved in toluene-d_8. The proportion observed was 74% HD and 26% H_2. However, the presence of HD and D_2 was not observed in toluene-H_8.

Procedure for the Catalytic Hydrogenation of CO_2. In a dry flask, solutions of KOH (0.1 M) and the corresponding precatalysts (50 μM) in 5 mL of H_2O were placed in a stainless steel autoclave. The autoclave was purged with CO_2 for 5 min. After 10 min of stabilization at the desired temperature, 10 bar of H_2/CO_2 (1/1) gas were introduced and the reaction was started with stirring (1500 rpm). The stirring was stopped after 3 or 8 h and the pressurized gas was released. An aliquot of 0.5 mL was taken from the resulting solutions, to which dioxane was added as a reference (0.0125 mol). The formate concentration was determined by ^1H NMR spectroscopy (after a previous calibration; see SI).

Procedures for the Characterization of Catalytic Intermediates by NMR. *1. Reactivity of Precatalysts with HCO_2Na.* In a dry NMR tube previously purged with nitrogen, a solution of the corresponding precatalyst (7.5×10^{-3} mmol) in D_2O (0.5 mL) was introduced. A ^1H NMR spectrum was recorded and then an excess of HCO_2Na was added (4.4 mg, 6.5×10^{-2} mmol). The evolution of the reaction with time was monitored by ^1H NMR spectroscopy.

In the case of **4**, one spectrum was registered each 10 min. Dioxane (1 μL, 0.011 mmol) was added as internal reference. The ^2D NMR spectrum was recorded after 48 h.

2. Reactivity of Precatalysts with DCl. In a dry NMR tube previously purged with nitrogen, a solution of the corresponding

DOI: 10.1021/acs.inorgchem.8b02164
Inorg. Chem. XXXX, XXX, XXX−XXX

precatalyst (7.5×10^{-3} mmol) in D_2O (0.5 mL) was introduced. A ^1H NMR spectrum was recorded and then a solution of DCl was added (1 M in D_2O, 50 μL). The evolution of the reaction with time was monitored by ^1H NMR spectroscopy.

3. Reactivity of the Precatalysts with Na_2CO_3. In a dry NMR tube previously purged with nitrogen, a solution of **3**, **4**, or **I** (7.5×10^{-3} mmol) in D_2O (0.5 mL) was introduced. A ^1H NMR spectrum was recorded and then Na_2CO_3 (1 mg, 9.5×10^{-3} mmol) was added. The evolution of the reaction with time was monitored by ^1H NMR spectoscopy.

■ ASSOCIATED CONTENT

Supporting Information

The Supporting Information is available free of charge on the ACS Publications website at DOI: 10.1021/acs.inorgchem.8b02164.

Molecular and crystalline structure; catalytic experiments and mechanistic studies (DOCX)

Accession Codes

CCDC 1858461 contains the supplementary crystallographic data for this paper. These data can be obtained free of charge via www.ccdc.cam.ac.uk/data_request/cif, or by emailing data_request@ccdc.cam.ac.uk, or by contacting The Cambridge Crystallographic Data Centre, 12 Union Road, Cambridge CB2 1EZ, UK; fax: +44 1223 336033.

■ AUTHOR INFORMATION

Corresponding Authors

*E-mail: gespino@ubu.es (G.E.).
*E-mail: Blanca.Manzano@uclm.es (B.R.M.).

ORCID

Gabriel García-Herbosa: 0000-0002-2863-1272
Félix A. Jalón: 0000-0002-6622-044X
Blanca R. Manzano: 0000-0002-4908-4503
Gustavo Espino: 0000-0001-5617-5705

Author Contributions

#These authors have contributed equally to the experimental part of this paper.

Notes

The authors declare no competing financial interest.

■ ACKNOWLEDGMENTS

We gratefully acknowledge the financial support provided by the Spanish Ministerio de Economía y Competitividad - FEDER (CTQ2014-58812-C2-1-R). M. R.-C. is grateful for the grant from University of Castilla-La Mancha (programa propio).

■ REFERENCES

(1) Chaloner, P. A.; Esteruelas, M. A.; Joó, F.; Oro, L. A. *Homogeneous Hydrogenation*; Kluwer Academic Publishers: Dordrecht, 1994.

(2) *Recent Advances in Hydride Chemistry*, Peruzzini, M.; Poli, R., Eds.; Elsevier: Amsterdam, 2001.

(3) Torrente-Murciano, L.; Mattia, D.; Jones, M. D.; Plucinski, P. K. Formation of Hydrocarbons via CO2 Hydrogenation − A Thermodynamic Study. *J. CO_2 Util.* **2014**, *6*, 34−39.

(4) Jiang, H. L.; Singh, S. K.; Yan, J. M.; Zhang, X. B.; Xu, Q. Liquid-Phase Chemical Hydrogen Storage: Catalytic Hydrogen Generation under Ambient Conditions. *ChemSusChem* **2010**, *3* (5), 541−549.

(5) Wang, W. H.; Himeda, Y.; Muckerman, J. T.; Manbeck, G. F.; Fujita, E. CO_2 Hydrogenation to Formate and Methanol as an Alternative to Photo- and Electrochemical CO_2 Reduction. *Chem. Rev.* **2015**, *115* (23), 12936−12973.

(6) Izumi, Y. Recent Advances in the Photocatalytic Conversion of Carbon Dioxide to Fuels with Water and/or Hydrogen Using Solar Energy and Beyond. *Coord. Chem. Rev.* **2013**, *257* (1), 171−186.

(7) Qiao, J.; Liu, Y.; Hong, F.; Zhang, J. A Review of Catalysts for the Electroreduction of Carbon Dioxide to Produce Low-Carbon Fuels. *Chem. Soc. Rev.* **2014**, *43*, 631.

(8) Zhang, W.; Hu, Y.; Ma, L.; Zhu, G.; Wang, Y.; Xue, X.; Chen, R.; Yang, S.; Jin, Z. Progress and Perspective of Electrocatalytic CO_2 Reduction for Renewable Carbonaceous Fuels and Chemicals. *Adv. Sci.* **2018**, *5* (1), 1700275.

(9) Centi, G.; Perathoner, S. Opportunities and Prospects in the Chemical Recycling of Carbon Dioxide to Fuels. *Catal. Today* **2009**, *148* (3−4), 191−205.

(10) Rand, D. A. J.; Dell, R. M. *Hydrogen Energy. Challenges and Prospects*; RSC Publishing: Cambridge, 2008.

(11) Liu, C.; Li, F.; Ma, L.-P.; Cheng, H.-M. Advanced Materials for Energy Storage. *Adv. Mater.* **2010**, *22* (8), E28−E62.

(12) Schlapbach, L.; Züttel, A. Hydrogen-Storage Materials for Mobile Applications. *Nature* **2001**, *414* (6861), 353−358.

(13) Johnson, T. C.; Morris, D. J.; Wills, M. Hydrogen Generation from Formic Acid and Alcohols Using Homogeneous Catalysts. *Chem. Soc. Rev.* **2010**, *39* (1), 81−88.

(14) Sordakis, K.; Tang, C.; Vogt, L. K.; Junge, H.; Dyson, P. J.; Beller, M.; Laurenczy, G. Homogeneous Catalysis for Sustainable Hydrogen Storage in Formic Acid and Alcohols. *Chem. Rev.* **2018**, *118* (2), 372−433.

(15) Onishi, N.; Xu, S.; Manaka, Y.; Suna, Y.; Wang, W. H.; Muckerman, J. T.; Fujita, E.; Himeda, Y. CO_2 Hydrogenation Catalyzed by Iridium Complexes with a Proton-Responsive Ligand. *Inorg. Chem.* **2015**, *54* (11), 5114−5123.

(16) Iglesias, M.; Oro, L. A. Mechanistic Considerations on Homogeneously Catalyzed Formic Acid Dehydrogenation. *Eur. J. Inorg. Chem.* **2018**, *2018*, 2125.

(17) Mellone, I.; Gorgas, N.; Bertini, F.; Peruzzini, M.; Kirchner, K.; Gonsalvi, L. Selective Formic Acid Dehydrogenation Catalyzed by Fe-PNP Pincer Complexes Based on the 2,6-Diaminopyridine Scaffold. *Organometallics* **2016**, *35* (19), 3344−3349.

(18) Bielinski, E. A.; Lagaditis, P. O.; Zhang, Y.; Mercado, B. Q.; Würtele, C.; Bernskoetter, W. H.; Hazari, N.; Schneider, S. Lewis Acid-Assisted Formic Acid Dehydrogenation Using a Pincer-Supported Iron Catalyst. *J. Am. Chem. Soc.* **2014**, *136* (29), 10234−10237.

(19) Boddien, A.; Loges, B.; Gärtner, F.; Torborg, C.; Fumino, K.; Junge, H.; Ludwig, R.; Beller, M. Iron-Catalyzed Hydrogen Production from Formic Acid. *J. Am. Chem. Soc.* **2010**, *132* (26), 8924−8934.

(20) Celaje, J. J. A.; Lu, Z.; Kedzie, E. A.; Terrile, N. J.; Lo, J. N.; Williams, T. J. A Prolific Catalyst for Dehydrogenation of Neat Formic Acid. *Nat. Commun.* **2016**, *7*, 11308.

(21) Wang, W. H.; Hull, J. F.; Muckerman, J. T.; Fujita, E.; Hirose, T.; Himeda, Y. Highly Efficient D_2 generation by Dehydrogenation of Formic Acid in D2O through H^+/D^+ exchange on an Iridium Catalyst: Application to the Synthesis of Deuterated Compounds by Transfer Deuterogenation. *Chem. - Eur. J.* **2012**, *18* (30), 9397−9404.

(22) Iturmendi, A.; Rubio-Pérez, L.; Pérez-Torrente, J. J.; Iglesias, M.; Oro, L. A. Impact of Protic Ligands in the Ir-Catalyzed Dehydrogenation of Formic Acid in Water. *Organometallics* **2018**, *37*, 3611.

(23) Wang, L.; Sun, H.; Zuo, Z.; Li, X.; Xu, W.; Langer, R.; Fuhr, O.; Fenske, D. Activation of CO_2, CS_2, and Dehydrogenation of Formic Acid Catalyzed by Iron(II) Hydride Complexes. *Eur. J. Inorg. Chem.* **2016**, *2016* (33), 5205−5214.

(24) Xiao, P.; Wu, D.; Fang, W.-H.; Cui, G. Mechanistic Insights into the Light-Driven Hydrogen Evolution Reaction from Formic Acid Mediated by an Iridium Photocatalyst. *Catal. Sci. Technol.* **2017**, *7* (13), 2763−2771.

DOI: 10.1021/acs.inorgchem.8b02164
Inorg. Chem. XXXX, XXX, XXX−XXX

(25) Boddien, A.; Mellmann, D.; Gärtner, F.; Jackstell, R.; Junge, H.; Dyson, P. J.; Laurenczy, G.; Ludwig, R.; Beller, M. Efficient Dehydrogenation of Formic. *Science (Washington, DC, U. S.)* **2011**, *333*, 1733−1737.
(26) Iguchi, M.; Himeda, Y.; Manaka, Y.; Kawanami, H. Development of an Iridium-Based Catalyst for High-Pressure Evolution of Hydrogen from Formic Acid. *ChemSusChem* **2016**, *9* (19), 2749−2753.
(27) Bertini, F.; Glatz, M.; Gorgas, N.; Stöger, B.; Peruzzini, M.; Veiros, L. F.; Kirchner, K.; Gonsalvi, L. Carbon Dioxide Hydrogenation Catalysed by Well-Defined Mn(i) PNP Pincer Hydride Complexes. *Chem. Sci.* **2017**, *8* (7), 5024−5029.
(28) Tanaka, R.; Yamashita, M.; Nozaki, K. Catalytic Hydrogenation of Carbon Dioxide Using Ir (III) -Pincer Complexes and Its Mechanistic Investigation. *J. Am. Chem. Soc.* **2009**, *131*, 14168−14169.
(29) Bertini, F.; Gorgas, N.; Stöger, B.; Peruzzini, M.; Veiros, L. F.; Kirchner, K.; Gonsalvi, L. Efficient and Mild Carbon Dioxide Hydrogenation to Formate Catalyzed by Fe(II) Hydrido Carbonyl Complexes Bearing 2,6-(Diaminopyridyl)Diphosphine Pincer Ligands. *ACS Catal.* **2016**, *6* (5), 2889−2893.
(30) Langer, R.; Diskin-Posner, Y.; Leitus, G.; Shimon, L. J. W.; Ben-David, Y.; Milstein, D. Low-Pressure Hydrogenation of Carbon Dioxide Catalyzed by an Iron Pincer Complex Exhibiting Noble Metal Activity. *Angew. Chem., Int. Ed.* **2011**, *50* (42), 9948−9952.
(31) Glüer, A.; Schneider, S. Iron Catalyzed Hydrogenation and Electrochemical Reduction of CO_2: The Role of Functional Ligands. *J. Organomet. Chem.* **2018**, *861*, 159−173.
(32) Wang, W.; Wang, S.; Ma, X.; Gong, J. Recent Advances in Catalytic Hydrogenation of Carbon Dioxide. *Chem. Soc. Rev.* **2011**, *40* (7), 3703−3727.
(33) Sanz, S.; Benítez, M.; Peris, E. A New Approach to the Reduction of Carbon Dioxide: CO_2 Reduction to Formate by Transfer Hydrogenation in IPrOH. *Organometallics* **2010**, *29* (1), 275−277.
(34) Himeda, Y.; Onozawa-Komatsuzaki, N.; Sugihara, H.; Arakawa, H.; Kasuga, K. Half-Sandwich Complexes with 4,7-Dihydroxy-1,10-Phenanthroline: Water-Soluble, Highly Efficient Catalysts for Hydrogenation of Bicarbonate Attributable to the Generation of an Oxyanion on the Catalyst Ligand. *Organometallics* **2004**, *23* (7), 1480−1483.
(35) Hull, J. F.; Himeda, Y.; Wang, W.-H.; Hashiguchi, B.; Periana, R.; Szalda, D. J.; Muckerman, J. T.; Fujita, E. Reversible Hydrogen Storage Using CO2 and a Proton-Switchable Iridium Catalyst in Aqueous Media under Mild Temperatures and Pressures. *Nat. Chem.* **2012**, *4* (5), 383−388.
(36) Gorgas, N.; Kirchner, K. Isoelectronic Manganese and Iron Hydrogenation/Dehydrogenation Catalysts: Similarities and Divergences. *Acc. Chem. Res.* **2018**, *51* (6), 1558−1569.
(37) Bernskoetter, W. H.; Hazari, N. Reversible Hydrogenation of Carbon Dioxide to Formic Acid and Methanol: Lewis Acid Enhancement of Base Metal Catalysts. *Acc. Chem. Res.* **2017**, *50* (4), 1049−1058.
(38) Tanaka, R.; Yamashita, M.; Chung, L. W.; Morokuma, K.; Nozaki, K. Mechanistic Studies on the Reversible Hydrogenation of Carbon Dioxide Catalyzed by an Ir-PNP Complex. *Organometallics* **2011**, *30* (24), 6742−6750.
(39) Bertini, F.; Mellone, I.; Ienco, A.; Peruzzini, M.; Gonsalvi, L. Iron(II) Complexes of the Linear Rac-Tetraphos-1 Ligand as Efficient Homogeneous Catalysts for Sodium Bicarbonate Hydrogenation and Formic Acid Dehydrogenation. *ACS Catal.* **2015**, *5* (2), 1254−1265.
(40) Gao, Y.; Kuncheria, J. K.; Jenkins, H. A.; Puddephatt, R. J.; Yap, G. The Interconversion of Formic Acid and Hydrogen/Carbon Dioxide Using a Binuclear Ruthenium Complex Catalyst. *J. Chem. Soc., Dalton Trans.* **2000**, *2* (18), 3212−3217.
(41) Geri, J. B.; Ciatti, J. L.; Szymczak, N. K. Charge Effects Regulate Reversible CO_2 Reduction Catalysis. *Chem. Commun.* **2018**, *54* (56), 7790−7793.
(42) Himeda, Y.; Miyazawa, S.; Hirose, T. Interconversion between Formic Acid and H_2/CO_2 Using Rhodium and Ruthenium Catalysts for CO_2 Fixation and H_2 Storage. *ChemSusChem* **2011**, *4* (4), 487−493.
(43) Filonenko, G. A.; Van Putten, R.; Schulpen, E. N.; Hensen, E. J. M.; Pidko, E. A. Highly Efficient Reversible Hydrogenation of Carbon Dioxide to Formates Using a Ruthenium PNP-Pincer Catalyst. *ChemCatChem* **2014**, *6* (6), 1526−1530.
(44) Maenaka, Y.; Suenobu, T.; Fukuzumi, S. Catalytic Interconversion between Hydrogen and Formic Acid at Ambient Temperature and Pressure. *Energy Environ. Sci.* **2012**, *5* (6), 7360−7367.
(45) Wei, Y.; Wu, X.; Wang, C.; Xiao, J. Transfer Hydrogenation in Aqueous Media. *Catal. Today* **2015**, *247*, 104−116.
(46) He, Y.-M.; Fan, Q.-H. Advances in Transfer Hydrogenation of Carbonyl Compounds in Water. *ChemCatChem* **2015**, *7* (3), 398−400.
(47) Wu, X.; Wang, C.; Xiao, J. Asymmetric Transfer Hydrogenation in Water with Platinum Group Metal Catalysts. *Platinum Met. Rev.* **2010**, *54* (1), 3−19.
(48) Wang, C.; Wu, X.; Xiao, J. Broader, Greener, and More Efficient: Recent Advances in Asymmetric Transfer Hydrogenation. *Chem. - Asian J.* **2008**, *3* (10), 1750−1770.
(49) Wu, X.; Xiao, J. Aqueous-Phase Asymmetric Transfer Hydrogenation of Ketones ? A Greener Approach to Chiral Alcohols. *Chem. Commun.* **2007**, 2449−2466.
(50) Fleury-Brégeot, N.; de la Fuente, V.; Castillón, S.; Claver, C. Highlights of Transition Metal-Catalyzed Asymmetric Hydrogenation of Imines. *ChemCatChem* **2010**, *2* (11), 1346−1371.
(51) Zhou, Y.-G. Asymmetric Hydrogenation of Heteroaromatic Compounds. *Acc. Chem. Res.* **2007**, *40* (12), 1357−1366.
(52) Wang, W. B.; Lu, S. M.; Yang, P. Y.; Han, X. W.; Zhou, Y. G. Highly Enantioselective Iridium-Catalyzed Hydrogenation of Heteroaromatic Compounds, Quinolines. *J. Am. Chem. Soc.* **2003**, *125* (35), 10536−10537.
(53) Wang, D. S.; Chen, Q. A.; Lu, S. M.; Zhou, Y. G. Asymmetric Hydrogenation of Heteroarenes and Arenes. *Chem. Rev.* **2012**, *112* (4), 2557−2590.
(54) Janiak, C. A Critical Account on Π−π Stacking in Metal Complexes with Aromatic Nitrogen-Containing Ligands. *J. Chem. Soc., Dalton Trans.* **2000**, 3885−3896.
(55) Katritzky, A. R.; Rachwal, S.; Rachwal, B. Recent Progress in the Synthesis of 1,2,2,4-Tetrahydroquinolines. *Tetrahedron* **1996**, *52* (48), 15031−15070.
(56) Tan, J.; Tang, W.; Sun, Y.; Jiang, Z.; Chen, F.; Xu, L.; Fan, Q.; Xiao, J. PH-Regulated Transfer Hydrogenation of Quinoxalines with a Cp*Ir-Diamine Catalyst in Aqueous Media. *Tetrahedron* **2011**, *67* (34), 6206−6213.
(57) Zhang, L.; Qiu, R.; Xue, X.; Pan, Y.; Xu, C.; Li, H.; Xu, L. Versatile (Pentamethylcyclopentadienyl)Rhodium-2,2′-Bipyridine (Cp*Rh-Bpy) Catalyst for Transfer Hydrogenation of N-Heterocycles in Water. *Adv. Synth. Catal.* **2015**, *357* (16−17), 3529−3537.
(58) Wang, C.; Li, C.; Wu, X.; Pettman, A.; Xiao, J. PH-Regulated Asymmetric Transfer Hydrogenation of Quinolines in Water. *Angew. Chem., Int. Ed.* **2009**, *48* (35), 6524−6528.
(59) Talwar, D.; Li, H. Y.; Durham, E.; Xiao, J. A Simple Iridicycle Catalyst for Efficient Transfer Hydrogenation of N-Heterocycles in Water. *Chem. - Eur. J.* **2015**, *21* (14), 5370−5379.
(60) Dobereiner, G. E.; Nova, A.; Schley, N. D.; Hazari, N.; Miller, S. J.; Eisenstein, O.; Crabtree, R. H. Iridium-Catalyzed Hydrogenation of N-Heterocyclic Compounds under Mild Conditions by an Outer-Sphere Pathway. *J. Am. Chem. Soc.* **2011**, *133* (19), 7547−7562.
(61) Yang, P. Y.; Zhou, Y. G. The Enantioselective Total Synthesis of Alkaloid (−)-Galipeine. *Tetrahedron: Asymmetry* **2004**, *15* (7), 1145−1149.
(62) Lu, S. M.; Han, X. W.; Zhou, Y. G. Asymmetric Hydrogenation of Quinolines Catalyzed by Iridium with Chiral Ferrocenyloxazoline Derived N,P Ligands. *Adv. Synth. Catal.* **2004**, *346* (8), 909−912.

DOI: 10.1021/acs.inorgchem.8b02164
Inorg. Chem. XXXX, XXX, XXX−XXX

(63) Reetz, M. T.; Li, X. Asymmetric Hydrogenation of Quinolines Catalyzed by Iridium Complexes of BINOL-Derived Diphosphonites. *Chem. Commun.* **2006**, *52* (20), 2159−2160.
(64) Lu, S. M.; Wang, Y. Q.; Han, X. W.; Zhou, Y. G. Asymmetric Hydrogenation of Quinolines and Isoquinolines Activated by Chloroformates. *Angew. Chem., Int. Ed.* **2006**, *45* (14), 2260−2263.
(65) Zhou, H.; Li, Z.; Wang, Z.; Wang, T.; Xu, L.; He, Y.; Fan, Q. H.; Pan, J.; Gu, L.; Chan, A. S. C. Hydrogenation of Quinolines Using a Recyclable Phosphine-Free Chiral Cationic Ruthenium Catalyst: Enhancement of Catalyst Stability and Selectivity in an Ionic Liquid. *Angew. Chem., Int. Ed.* **2008**, *47* (44), 8464−8467.
(66) Li, Z. W.; Wang, T. L.; He, Y. M.; Wang, Z. J.; Fan, Q. H.; Pan, J.; Xu, L. J. Air-Stable and Phosphine-Free Iridium Catalysts for Highly Enantioselective Hydrogenation of Quinoline Derivatives. *Org. Lett.* **2008**, *10* (22), 5265−5268.
(67) Xu, L.; Lam, K. H.; Ji, J.; Wu, J.; Fan, Q.-H.; Lo, W.-H.; Chan, A. S. C. Air-Stable Ir-(P-Phos) Complex for Highly Enantioselective Hydrogenation of Quinolines and Their Immobilization in Poly-(Ethylene Glycol) Dimethyl Ether (DMPEG). *Chem. Commun.* **2005**, 1390−1392.
(68) Yamaguchi, R.; Ikeda, C.; Takahashi, Y.; Fujita, K. I. Homogeneous Catalytic System for Reversible Dehydrogenation-Hydrogenation Reactions of Nitrogen Heterocycles with Reversible Interconversion of Catalytic Species. *J. Am. Chem. Soc.* **2009**, *131* (24), 8410−8412.
(69) Crabtree, R. H. Multifunctional Ligands in Transition Metal Catalysis. *New J. Chem.* **2011**, *35* (1), 18−23.
(70) Rakowski DuBois, M.; DuBois, D. L. The Roles of the First and Second Coordination Spheres in the Design of Molecular Catalysts for H 2 Production and Oxidation. *Chem. Soc. Rev.* **2009**, *38* (1), 62−72.
(71) Schmeier, T. J.; Dobereiner, G. E.; Crabtree, R. H.; Hazari, N. Secondary Coordination Sphere Interactions Facilitate the Insertion. *J. Am. Chem. Soc.* **2011**, *133* (24), 9274−9277.
(72) Barnard, J. H.; Wang, C.; Berry, N. G.; Xiao, J. Long-Range Metal−ligand Bifunctional Catalysis: Cyclometallated Iridium Catalysts for the Mild and Rapid Dehydrogenation of Formic Acid. *Chem. Sci.* **2013**, *4* (3), 1234.
(73) Türkmen, H.; Kani, I.; Çetinkaya, B. Transfer Hydrogenation of Aryl Ketones with Half-Sandwich Ru II Complexes That Contain Chelating Diamines. *Eur. J. Inorg. Chem.* **2012**, *2012*, 4494−4499.
(74) Gupta, K.; Tyagi, D.; Dwivedi, A. D.; Mobin, S. M.; Singh, S. K. Catalytic Transformation of Bio-Derived Furans to Valuable Ketoacids and Diketones by Water-Soluble Ruthenium Catalysts. *Green Chem.* **2015**, *17* (9), 4618−4627.
(75) Carrión, M. C.; Jalón, F. A.; Manzano, B. R.; Rodríguez, A. M.; Sepúlveda, F.; Maestro, M. (Arene)Ruthenium(II) Complexes Containing Substituted Bis(Pyrazolyl)Methane Ligands - Catalytic Behaviour in Transfer Hydrogenation of Ketones. *Eur. J. Inorg. Chem.* **2007**, *2007* (25), 3961−3973.
(76) Carrión, M. C.; Sepúlveda, F.; Jalón, F. A.; Manzano, B. R.; Rodríguez, A. M. Base-Free Transfer Hydrogenation of Ketones Using Arene Ruthenium(II) Complexes. *Organometallics* **2009**, *28* (13), 3822−3833.
(77) Espino, G.; Caballero, A.; Manzano, B. R.; Santos, L.; Pérez-Manrique, M.; Moreno, M.; Jalón, F. A. Experimental and Computational Evidence for the Participation of Nonclassical Dihydrogen Species in Proton Transfer Processes on Ru−Arene Complexes with Uncoordinated N Centers. Efficient Catalytic Deuterium Labeling of H 2 with CD 3 OD. *Organometallics* **2012**, *31* (8), 3087−3100.
(78) Martínez, M.; Carranza, M. P.; Massaguer, A.; Santos, L.; Organero, J. A.; Aliende, C.; De Llorens, R.; Ng-Choi, I.; Feliu, L.; Planas, M.; et al. Synthesis and Biological Evaluation of Ru(II) and Pt(II) Complexes Bearing Carboxyl Groups as Potential Anticancer Targeted Drugs. *Inorg. Chem.* **2017**, *56* (22), 13679−13696.
(79) Chong, C. C.; Kinjo, R. Hydrophosphination of CO2 and Subsequent Formate Transfer in the 1,3,2-Diazaphospholene-Catalyzed N-Formylation of Amines. *Angew. Chem., Int. Ed.* **2015**, *54* (41), 12116−12120.
(80) Zhao, T.-X.; Zhai, G.-W.; Liang, J.; Li, P.; Hu, X.-B.; Wu, Y.-T. Catalyst-Free N-Formylation of Amines Using BH_3NH_3 and CO_2 under Mild Conditions. *Chem. Commun.* **2017**, *53* (57), 8046−8049.
(81) Shah, N.; Gravel, E.; Jawale, D. V.; Doris, E.; Namboothiri, I. N. N. Carbon Nanotube-Gold Nanohybrid Catalyzed N-Formylation of Amines by Using Aqueous Formaldehyde. *ChemCatChem* **2014**, *6* (8), 2201−2205.
(82) Hulla, M.; Bobbink, F. D.; Das, S.; Dyson, P. J. Carbon Dioxide Based N-Formylation of Amines Catalyzed by Fluoride and Hydroxide Anions. *ChemCatChem* **2016**, *8* (21), 3338−3342.
(83) Zheng, D.; Zhou, X.; Cui, B.; Han, W.; Wan, N.; Chen, Y. Biocatalytic α-Oxidation of Cyclic Amines and N-Methylanilines for the Synthesis of Lactams and Formamides. *ChemCatChem* **2017**, *9* (6), 937−940.
(84) Rahman, S.; Fukamiya, N.; Okano, M.; Tagahara, K.; Lee, K.-H. NII-Electronic Library Service. *Chem. Pharm. Bull.* **1997**, *45* (9), 1527−1529.
(85) Chen, F.; Sahoo, B.; Kreyenschulte, C.; Lund, H.; Zeng, M.; He, L.; Junge, K.; Beller, M. Selective Cobalt Nanoparticles for Catalytic Transfer Hydrogenation of N-Heteroarenes. *Chem. Sci.* **2017**, *8* (9), 6239−6246.
(86) Tao, L.; Zhang, Q.; Li, S. S.; Liu, X.; Liu, Y. M.; Cao, Y. Heterogeneous Gold-Catalyzed Selective Reductive Transformation of Quinolines with Formic Acid. *Adv. Synth. Catal.* **2015**, *357* (4), 753−760.
(87) Vilhanová, B.; van Bokhoven, J. A.; Ranocchiari, M. Gold Particles Supported on Amino-Functionalized Silica Catalyze Transfer Hydrogenation of N-Heterocyclic Compounds. *Adv. Synth. Catal.* **2017**, *359* (4), 677−686.
(88) Zhang, J. F.; Zhong, R.; Zhou, Q.; Hong, X.; Huang, S.; Cui, H. Z.; Hou, X. F. Recyclable Silica-Supported Iridium Catalysts for Selective Reductive Transformation of Quinolines with Formic Acid in Water. *ChemCatChem* **2017**, *9* (13), 2496−2505.
(89) Saari, W. S.; Halczenko, W.; Freedman, M. B.; Arison, B. H. Synthesis and Reactions of Some Dihydro and Tetrahydro-4H-Imidazo[5,4,l-Ij]Quinoline Derivatives. *J. Heterocycl. Chem.* **1982**, *19*, 837−840.
(90) Shugrue, C. R.; Miller, S. J. Phosphothreonine as a Catalytic Residue in Peptide-Mediated Asymmetric Transfer Hydrogenations of 8-Aminoquinolines. *Angew. Chem., Int. Ed.* **2015**, *54* (38), 11173−11176.
(91) Yamaguchi, R.; Ikeda, C.; Takahashi, Y.; Fujita, K.-I. *J. Am. Chem. Soc.* **2009**, *131*, 8410−8412.
(92) Wu, J.; Talwar, D.; Johnston, S.; Yan, M.; Xiao, J. Acceptorless Dehydrogenation of Nitrogen Heterocycles with a Versatile Iridium Catalyst. *Angew. Chem., Int. Ed.* **2013**, *52* (27), 6983−6987.
(93) Carrión, M. C.; Ruiz-Castañeda, M.; Espino, G.; Aliende, C.; Santos, L.; Rodríguez, A. M.; Manzano, B. R.; Jalón, F. A.; Lledós, A. Selective Catalytic Deuterium Labeling of Alcohols during a Transfer Hydrogenation Process of Ketones Using D 2 O as the Only Deuterium Source. Theoretical and Experimental Demonstration of a Ru−H/D + Exchange as the Key Step. *ACS Catal.* **2014**, *4* (4), 1040−1053.
(94) Miyake, H.; Kano, N.; Kawashima, T. Isolation of a Metastable Geometrical Isomer of a Hexacoordinated Dihydrophosphate: Elucidation of Its Enhanced Reactivity in Umpolung of a Hydrogen Atom of Water. *Inorg. Chem.* **2011**, *50* (18), 9083−9089.
(95) Wang, W. H.; Hull, J. F.; Muckerman, J. T.; Fujita, E.; Hirose, T.; Himeda, Y. Highly Efficient D2 Generation by Dehydrogenation of Formic Acid in D2O through H+/D+ Exchange on an Iridium Catalyst: Application to the Synthesis of Deuterated Compounds by Transfer Deuterogenation. *Chem. - Eur. J.* **2012**, *18* (30), 9397−9404.
(96) Ohkuma, T.; Utsumi, N.; Tsutsumi, K.; Murata, K.; Sandoval, C.; Noyori, R. The Hydrogenation/Transfer Hydrogenation Network : Asymmetric Hydrogenation of Ketones with Chiral η 6 -Arene/N-Tosylethylenediamine-Ruthenium (II) Catalysts. *J. Am. Chem. Soc.* **2006**, *128* (27), 8724−8725.

DOI: 10.1021/acs.inorgchem.8b02164
Inorg. Chem. XXXX, XXX, XXX−XXX

(97) Bennett, M. A.; Smith, A. K. Arene Ruthenium(II) Complexes Formed by Dehydrogenation of Cyclohexadienes with Ruthenium-(III) Trichloride. *J. Chem. Soc., Dalton Trans.* **1974**, 233.
(98) Kang, J. W.; Moseley, K.; Maitlis, P. M. *J. Am. Chem. Soc.* **1969**, *91* (13), 5970−5977.
(99) Yates, A.; Maitlis, P. M. *Inorg. Synthesis* **1992**, *29*, 228−234.
(100) Fulmer, G. R.; Miller, A. J. M.; Sherden, N. H.; Gottlieb, H. E.; Nudelman, A.; Stoltz, B. M.; Bercaw, J. E.; Goldberg, K. I. NMR Chemical Shifts of Trace Impurities: Common Laboratory Solvents, Organics, and Gases in Deuterated Solvents Relevant to the Organometallic Chemist. *Organometallics* **2010**, *29* (9), 2176−2179.
(101) *SAINT* v 8.37 and *APEX3* v 2016.1.0. Bruker-AXS: Madison, WI, USA; 2016.
(102) Krause, L.; Herbst-Irmer, R.; Sheldrick, G. M.; Stalke, D. Comparison of Silver and Molybdenum Microfocus X-Ray Sources for Single-Crystal Structure Determination. *J. Appl. Crystallogr.* **2015**, *48* (1), 3−10.
(103) Farrugia, L. J. WinGX and ORTEP for Windows: An Update. *J. Appl. Crystallogr.* **2012**, *45* (4), 849−854.
(104) Sheldrick, G. M. *SHELX-2014: Progressive Crystal Structure Refinement*; University of Göttingen: Göttingen, Germany., 2014.

DOI: 10.1021/acs.inorgchem.8b02164
Inorg. Chem. XXXX, XXX, XXX−XXX